Using Radiation Thermometry to Assess Spatial Variation of Water Stressed Cotton

Susan A. O'Shaughnessy, Agricultural Engineer
USDA-ARS, P.O. Drawer 10, Bushland, TX, 79012
Susan.OShaughnessy@ARS.USDA.GOV

Steven R. Evett, Soil Scientist
USDA-ARS, P.O. Drawer 10, Bushland, TX, 79012
Steve.Evett@ARS.USDA.GOV

Abstract. *The use of infrared thermometry and thermal imagery to investigate unapparent but important field conditions (poor drainage, non-uniform irrigation, soil variability, or biotic infestations) offers a producer improved management tools to avoid yield declines or variability in crop status. This study investigated spatial and temporal crop water stress based on crop canopy temperature extracted from remote thermal images and point infrared thermometry within the imaged area to calculate an empirical crop water stress index ($CWSI_e$) for varying levels of manually and automatically irrigated cotton (Gossypium hirsutum L.). The daily $CWSI_e$ calculated from canopy temperature data extracted from thermal imagery was significantly related to midday leaf water potential (LWP), $r^2 = 0.88$ in 2007 and $r^2 = 0.77$ in 2008. Data from 2007 indicated a significant inverse correlation between seasonal mean $CWSI_e$ values derived from infrared thermometry and yields, $r^2 = 0.86$ and 0.77, $p < 0.001$, for manually and automatically irrigated plots, respectively. In 2008, there was also an inverse linear relationship between $CWSI_e$ and yield for deficit irrigated cotton in the automatic blocks, $r^2 = 1.0$, $p < 0.001$. However, there was a positive correlation between $CWSI_e$ and yields in the manually irrigated plots. High temperatures and wind, and heavy rainfall near the period of boll maturation negatively impacted yields and the yield – $CWSI_e$ relationship. In the future, it is plausible that thermal imaging sensors combined with computational analysis will provide real-time spatial and temporal information concerning in-field crop water status.*

Keywords. Infrared thermometry, infrared imaging, crop water stress, spatial variation

Introduction

Remote sensing technologies have potential as tools for monitoring crop water status, improving water use efficiency, saving water, and precisely managing irrigation. Useful information on canopy water relations can be derived from infrared thermometry and thermography. Infrared thermography in agriculture has been used as a non-invasive versatile imaging tool to investigate biotic stress (disease or insect infestation), and abiotic stresses (e.g., nutrient and water deficit). Chaerle et al. (2006) combined thermal and chlorophyll fluorescence imaging to study spatial and temporal heterogeneity of leaf transpiration and photosynthesis. These techniques helped them to identify pre-symptomatic responses (higher chlorophyll intensity co-located with thermal symptoms) and provided diagnosis of diseases (fungal and bacterial infections) and abiotic stresses not yet perceptible in visible spectrum images. Stoll et al. (2008) used an infrared camera to observe thermal responses in grapevine infected with a fungus well in advance of visible symptoms.

Studies involving the analysis of abiotic stresses with thermal imagery include those by Jones (1999) and Jones et al. (2002) in which field studies were designed to assess the consistency and repeatability of using thermal imagery to measure stomatal conductance in grapevine canopies. They concluded that thermography allows for semi-automated analysis of large areas of canopy with much more effective replication than can be achieved with porometry. Leinonen and Jones (2004) classified thermal images to identify leaf area, and sunlit and shaded parts of the canopy. Their methods provided improved estimates of temperature distribution across a canopy by separating out mixed pixels and reducing the effects of thermal contribution from background. Möeller et al. (2007) used thermal and visible imagery to estimate the crop water status of irrigated wine grapes. Their tactic included using the temperature of an artificial wet reference to estimate a wet baseline (i.e., a surrogate for a fully transpiring leaf) and using the maximum daily air temperature to estimate a dry baseline, both of which were needed to calculate a crop water stress index (CWSI) value that was then related to LWP. Ben-Gal et al. (2009) evaluated water stress in irrigated olive orchards using remote thermal imagery to measure average crop canopy temperature and calculate the CWSI using an empirical and analytical approach. It was determined that there was no significant difference between the two approaches.

At the Bushland USDA-ARS Conservation and Production Research Laboratory, thermal imagery has been used to document the spatial variability of crop water status, separate temperature contributions from sunlit and shaded plants and soil, document temperature differences between drying grain and plant leaves, and estimate crop canopy cover in irrigated fields. An empirical crop water stress index, $CWSI_e$, was calculated as:

$$\mathrm{CWSI}_e = \frac{T_c - T_w}{T_{dry} - T_w} \qquad [1]$$

where T_c was the temperature (°C) of the crop at the time of the thermometric image, T_w was the average temperature of a "wet reference" that acted as a substitute for the well-watered base line or lower boundary temperature. T_{dry} represented the upper boundary temperature and was estimated by adding 5°C to the maximum dry bulb temperature recorded (Möller et al., 2006) for the specific field day. This index ranges from > 0.0 since T_c is typically greater than T_{wet}, and can exceed 1.0 when the $T_c > T_{dry}$.

Additionally, infrared thermometers (IRTs) mounted on a center pivot irrigation system lateral have been used to remotely monitor soybean and cotton crop canopy temperature, and schedule automatic irrigations based on a thermal stress index (Peters and Evett, 2004). Our objective was to characterize in-field crop water status and estimate yields based on the $CWSI_e$. Initially temperatures extracted from the thermal imagery were used to calculate the stress index and compared to LWP. Scaled crop canopy temperature data (Peters and Evett, 2004) from the IRTs on the center pivot were used to formulate mean seasonal $CWSI_e$ values.

Methods and Materials

Agronomy

Crop water status was controlled spatially by full and deficit irrigations applied to a semi-circle of concentric plots blocked arc-wise by irrigation method, either manual or automatic scheduling techniques (Fig. 1). Cotton (*Gossypium hirsutum* L.), variety Paymaster 2280[1] was planted on day of year (DOY) 149 (May 29) in 2007 and variety Delta Pine 117 B2RF[1] was planted on DOY 141 in 2008 (both varieties were Bollgard II® Roundup Ready®, Delta and Pine Land Co., Scott, Miss.). The crops were grown in eighteen row plots on beds spaced 0.76-m apart under a three span center pivot at Bushland, Texas (35° 11' N, 102° 06' W, 1174 m above mean sea level). Manual irrigations were applied weekly to three blocks, each comprised of four treatment plots and two replicates (Fig. 1). Irrigation was applied manually at levels of 33%, 67%, and 100% (treatments designated $I_{33\%}$, $I_{67\%}$ and $I_{100\%}$) of full replenishment of soil water in the root zone to field capacity based on neutron moisture meter readings and using low energy precision application (LEPA) drag socks. Dryland plots were also included as the fourth treatment ($I_{0\%}$). Irrigation treatments were applied in the northwest half of the field in 2008 and the southeast half of the field in 2007 with the unused half of the field supporting a cover crop each year in order to even out soil water differences caused by the irrigation treatments in the year before. The blocks labeled "auto" were irrigated using the time-temperature threshold (TTT) algorithms for irrigation automation and control that use canopy temperature measurements (Peters and Evett, 2004). The full irrigation level for automatic treatments was based on the peak week-long crop water use, previously evaluated at Bushland as 10 mm d^{-1}. Each time a TTT irrigation signal was recorded, a 20-mm irrigation was automatically applied (double the peak water use because automatic irrigations were applied only every other day so that manual irrigations could be scheduled on alternate days). A temperature and humidity sensor (model Vaisala HMP45C, Campbell Scientific, Logan, Utah) was mounted at the end of the pivot arm and wired to a data logger (model CR10X, Campbell Scientific, Logan, Utah). Data were sampled every 10 sec and averaged and stored every minute. From these, the maximum dry bulb temperature was extracted each day the pivot moved for the calculation of T_{dry}.

---

[1] Mention of trade names or commercial products in this paper is solely for the purpose of providing specific information and does not imply recommendation or endorsement by the U.S. Department of Agriculture.

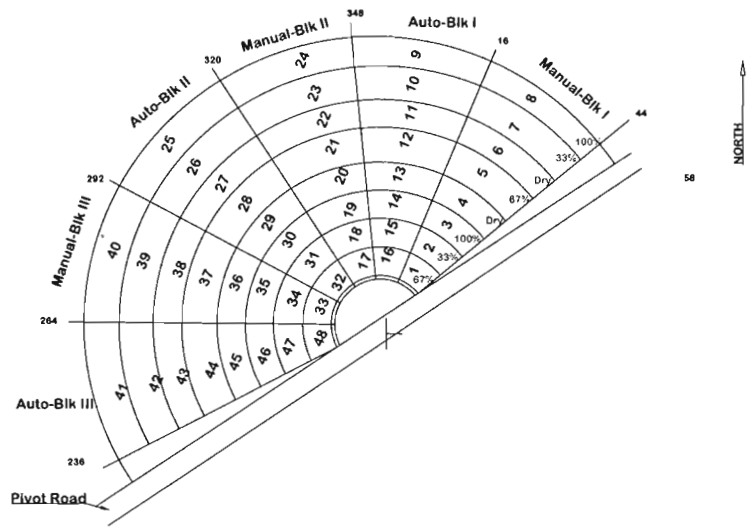

(a)

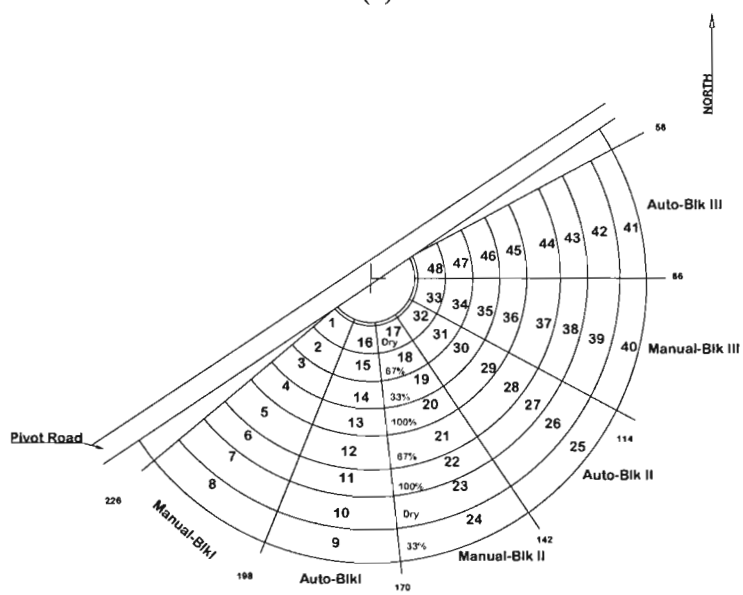

(b)

Figure 1. Experimental layout under the 3-span center pivot irrigation system shown for the (a) 2008 growing season; and (b) the 2007 growing season. Sections were blocked by irrigation method (manual versus automatic) with each block containing two replicates of the four irrigation level treatments, 100%, 67% and 33% and dryland (Dry).

Thermometric Measurements and Image Analysis

Digital images were taken with a thermal infrared camera and processed with corresponding software (model SC2000 and ThermaCAM Researcher Pro 2.8 software, FLIR Systems, Billerica, Mass.) on DOY 223 (Aug. 11), 240 (Aug. 28), 247 (Sept. 4), and 256 (Sept. 13) 2007, and on DOY 213 (July 31) and 261 (Sept. 17), 2008, near solar noon. Concurrent images were taken with an RGB digital camera (model DSC-S85, Sony Electronics, Inc., Oradell, N.J.) mounted alongside the thermal imager to aid in image analysis. Images were taken at a nadir view angle from a hydraulic platform 7.0 m above the ground over treatment plots 1-8 (Fig. 1), covering all four irrigation levels. For each thermometric image acquisition, cardboard crosses covered with aluminum foil were placed in the plant canopy to define the boundaries of interest. The crosses appeared as colder areas in the thermometric images and as bright areas in the RGB images. Canopy temperature for the $CWSI_e$ was determined by measurement of individual leaves secured to cardboard circles that were also covered with aluminum foil for easy discrimination; the leaves were fully expanded and sunlit. The wet reference was a 27 by 42 cm wet surface constructed from semi-permeable plastic foam blocks covered with white polyester felt resting in a basin filled with deionized water. The foam blocks and felt were submerged to re-wet them at least one min before readings were taken. Capillary action kept the fabric wetted for several minutes. The extracted wet reference temperatures, T_w, were average values of the unshaded areas of the wet reference. The digital photographs were used to improve digital analysis (Fig. 2b). The $CWSI_e$ was calculated with Eq. [1].

Whole field thermographic scans, taken from the hydraulic lift with the thermal imager, were used to calculate the $CWSI_e$ with Eq. [1] using the canopy temperature, T_c, from the image, the value of T_{dry} determined from maximum air temperature and RH data, and the value of T_{wet} from the wet reference.

Plant measurements

In order to characterize crop water stress, a widely accepted method of assessment was used, measurement of LWP, (Turner, 1988). Ten leaf stem water potential samples were taken from each treatment plot, 1-8, on each sampling day near solar noon. Leaves were excised with a razor blade, wrapped in aluminum foil, and placed in an ice chest until the petiole was inserted into the pressure chamber. All readings were performed within one hour of excision. Leaf water potential measurements were regressed against $CWSI_e$ values from corresponding treatment plots.

Infrared thermometry and field-wide $CWSI_e$ determinations

Sixteen infrared thermometer thermocouples (Exergen model IRT/c.5, Watertown, Mass.) with a 5:1 field of view were mounted on masts attached to the center pivot lateral, with two sensors facing into each treatment plot pointed towards the canopy at an oblique angle. One sensor was mounted at the outside edge of each plot and one sensor on the inside edge so that the sensors were aimed nearly towards each other from opposite sides of the plot, thus reducing sun angle effects. IRTs mounted on fixed masts in the fully irrigated treatment plots were used to record the diel variation of canopy temperature for use as the reference temperatures in the temperature scaling method of Peters and Evett (2004). Signals from these sensors were measured and recorded every 10 seconds and averaged and stored for each minute.

Average seasonal $CWSI_e$ values for each of the 48 plots were calculated from data measured on the days the pivot moved using scaled canopy temperatures (T_s) determined for 12:00 pm, CST (Peters and Evett, 2004 and 2008):

$$T_s = T_e + \frac{(T_{rmt,t} - T_e)(T_{ref} - T_e)}{T_{ref,t} - T_e} \qquad [2]$$

where T_e (°C) was the predawn canopy temperature; T_{ref} (°C) was the reference canopy temperature at the same time interval as T_s (°C) (i.e., 12:00 pm); $T_{rmt,t}$ was the one-time-of-day canopy temperature measurement at the plot (remote location, rmt) at any daylight time t, measured by the IRTs on the pivot arm; and $T_{ref,t}$ (°C) was the measured reference temperature for the time t that the plot (remote) temperature measurement was taken. Mean scaled canopy temperature measurements, T_s, for each treatment plot, were substituted for crop canopy temperature, T_c, in Eq. [1]; the $CWSI_e$ was calculated using T_{dry} = maximum daily dry-bulb temperature (T_{max}) + 5°C, and the wet reference temperature (T_w) estimated using:

$$T_w \approx T_a - \frac{e_s(T_a) - e_a}{\Delta + \gamma} \qquad [3]$$

where T_a was the air temperature (°C) at 12:00 pm, e_s is saturated vapor pressure (Pa) at T_a, and e_a is actual vapor pressure (Pa), Δ is slope of the saturated vapor pressure versus temperature curve (Pa °C^{-1}) evaluated at $(T_a + T_w)/2$, and γ is the psychometric constant (Pa °C^{-1}) (Alves et al., 2001).

Results:

Detailed surface temperature data were recorded by thermography as illustrated in Figure 2. Shaded soil temperatures were approximately 42°C, sunlit soil was > 50°C,

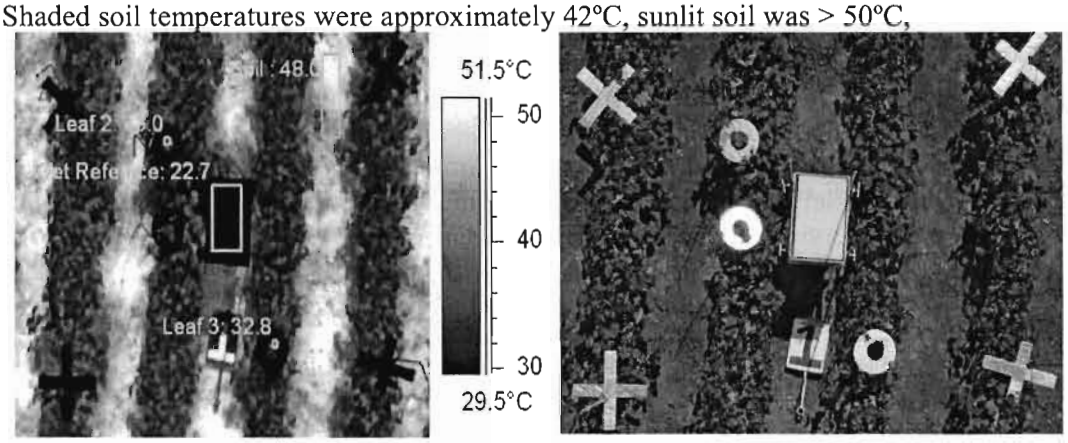

(a) (b)

Figure 2. Images taken from 7.0 m above a dryland plot: (a) thermal images of dryland cotton plot, showing average temperature of wet reference, soil, and individual leaves; (b) RBG digital images with wet reference in the center furrow. Photos were taken Sept 13, 2007.

average crop canopy temperature was approximately 32°C, and the wet reference

temperature was 22.7°C for this example. The $CWSI_e$ (0.51 for $I_{100\%}$, 0.64 for $I_{67\%}$, 0.78 for $I_{33\%}$, and 1.08 for $I_{0\%}$) derived from temperature data extracted from the whole-field thermal image where furrows are not visible (Fig. 3) provided a qualitative summary comparable to the trend

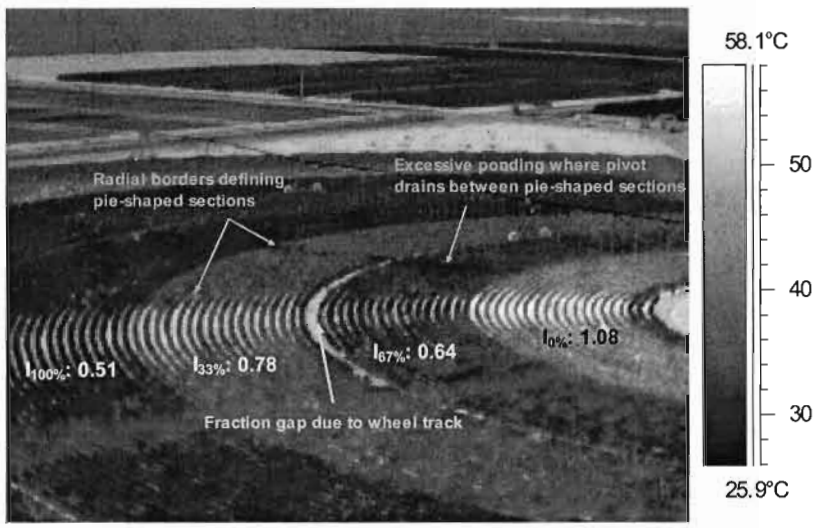

Figure 3. Whole-field image of the cotton field under the 3-span center pivot irrigation system showing the inner four concentric treatment plots ($I_{100\%}$, $I_{33\%}$, $I_{67\%}$, and $I_{0\%}$) and the corresponding values of CWSIe (0.51, 0.78, 0.64, and 1.08, respectively). Thermal image taken at Bushland, TX, on DOY 213 (Jul 31) in 2008.

shown in Table 1; the $CWSI_e$ decreases as the irrigation level increases. For accuracy comparable to that obtained from our nadir views, which showed individual leaves, data from whole field images should be digitally processed to normalize the impact of sun angle, percent fraction of vegetation, percent sunlit versus shaded components, and angle of view (Luquet et al., 2003).

Table 1. The CWSIe calculated using temperature data extracted from thermal images over individual treatment plots.

2007	Sampling date (DOY)			
Irrigation Treatment	223	240	247	256
0	0.32	0.88	0.85	0.57
33	0.32	0.87	0.77	0.66
67	0.17	0.79	0.56	0.46
100	0.11	0.71	0.48	0.35
2008	**Sampling date (DOY)**			
Irrigation Treatment	213		261	
0	0.75		0.77	
33	0.56		0.88	
67	0.28		0.81	
100	0.17		0.70	

Simple linear regression of the calculated *CWSI*$_e$, using data extracted from nadir thermal imagery, against leaf water potential measurements demonstrated a strong inverse linear relationship ($r^2 = 0.88$ in 2007; and $r^2 = 0.77$ in 2008). This confirmed that the *CWSI*$_e$ was a good indicator of in-field crop water stress (Fig. 4).

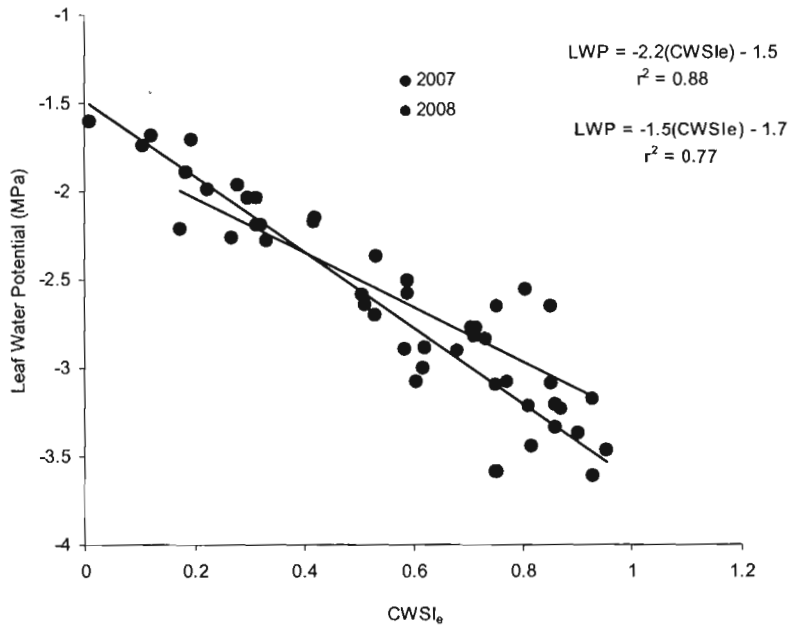

Figure 4. Plot showing the inverse relationship between leaf water potential and the empirical crop water stress index, $CWSI_e$, calculated using an artificial wet reference. Temperature and in situ measurements were made at mid-day during the 2007 and 2008 growing seasons.

These results prompted investigation of the $CWSI_e$ to characterize spatial variability of crop yield for all treatment plots under the center pivot for cotton grown in 2007 and 2008. The plot seasonal mean *CWSI*$_e$ explained 86% and 77% of the variation in the manually and automatically irrigated cotton yields, respectively, for the forty-eight treatment plots in 2007 (Fig. 5a and 5b). These results indicated a linear inverse relationship between the *CWSI*$_e$ and yields. The linear relationship between lint yield and the seasonal mean *CWSI*$_e$ in 2007 was similar to the lint yield relationships reported by Reginato (1983), LY = -1.96(CWSI) + 1.8, and Howell et al. (1984), LY = -1.91(CWSI) + 1.8, for conventional row cotton with 1.0 m spacing, where LY is lint yield and CWSI was calculated using the empirical method by Idso et al. (1981). Similar strongly significant inverse relationships were found by Peters and Evett (2007) between soybean yield, biomass, and total water use versus a seasonal plot mean standardized scaled temperature.

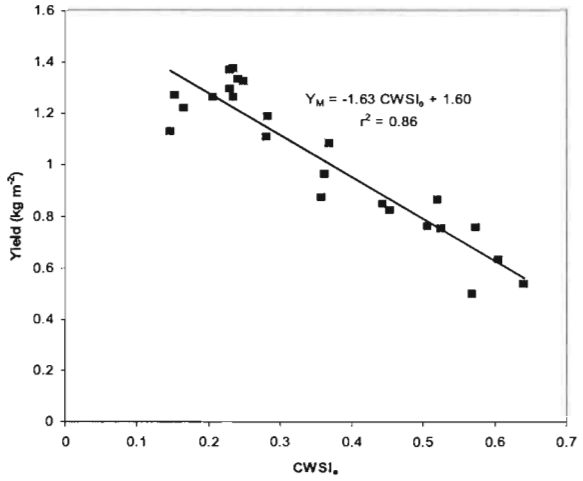

(a)

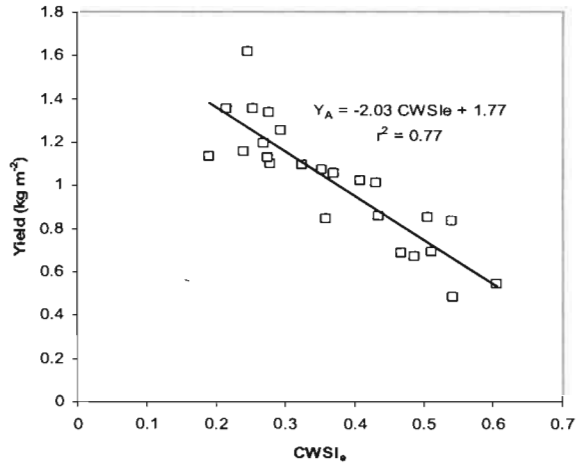

(b)

Figure 5. The inverse linear correlation between the empirical crop water stress index, $CWSI_e$, and yields for both: (a) manually and (b) automatically irrigated plots, 2007.

In 2008, the $CWSI_e$ values for the automatic-deficit irrigated plots were inversely correlated to yields (Fig. 6a) when data from the fully irrigated plots ($I_{100\%}$) were treated as an outlier. This is similar to the trend in 2007. However, for the manually irrigated plots, there existed a strong positive linear correlation between the $CWSI_e$ and the corresponding manually irrigated yields (Fig. 6b), when the dryland data was treated as an outlier. This relationship indicated that water-stressed cotton produced greater yields than well-irrigated cotton.

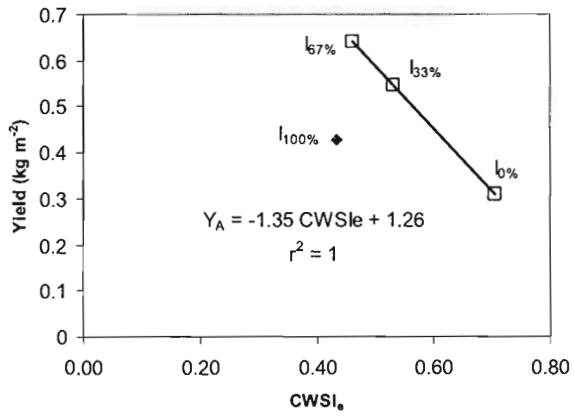

(a)

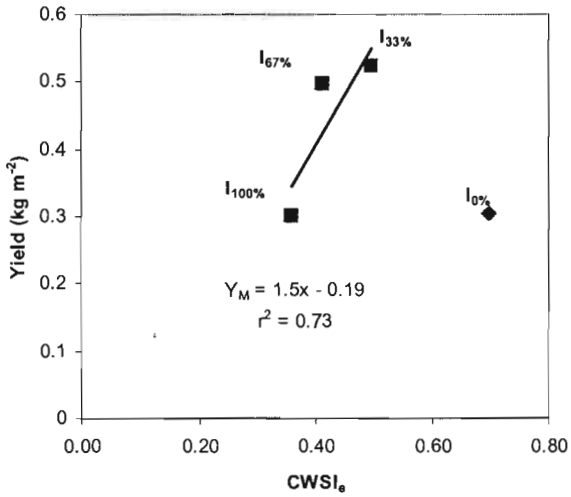

(b)

Figure 6. Cotton yields versus the empirical crop water stress index (CWSIe) for 2008: (a) automatic irrigations; and (b) manual irrigations. Each data point represents the average values from 6 treatment plots.

Mean values for the $CWSI_e$ and yields were used due to variability among individual treatment plots for both the manual and automatic irrigation methods. Overall, cotton production in 2008 was affected by high temperatures and windy conditions at emergence and heavy rainfall in mid August; reducing yields by 70% (data not shown).

Summary and Conclusion

In this study, it was demonstrated that whole-field canopy thermal images provide important qualitative information regarding spatial and temporal crop water status. Nadir thermal images offered detailed canopy temperature data, and an empirical CWSI calculated from thermal

images was significantly correlated to concurrent midday leaf water potential measurements. Seasonal plot mean values of $CWSI_e$ were also significantly correlated to crop yield during the 2007 growing season. Because the $CWSI_e$ requires minimal supplementary inputs to provide information on crop water status within a field, it is an inexpensive method of providing feedback to a producer. These early results demonstrated the potential positive impact of infrared thermography and remote canopy temperature sensing on farm management and their end-use as a tool for crop water stress monitoring and yield prediction. Infrared thermography could be used to scan an entire pivot field independent of pivot movement. However, fraction of vegetation, view angle, and cloud cover need to be taken into account. Methods are needed to automate the conversion of field infrared imagery to spatial maps for irrigation scheduling and site specific delivery of water. As thermal imagers become more affordable, automated digital analysis of field imagery taken at different times of the day and converted to useful and easily accessible data could provide decision support information to a producer and a means for improved irrigation and time management. Future studies are needed to evaluate the consistency of the $CWSI_e$'s usefulness during different growing seasons.

Acknowledgements

The authors appreciate the dedicated work performed by Brice Ruthardt, Biological Science Technician, USDA-ARS, Bushland, TX, and funding for this project from the Texas BARD program (grant no. TIE04-01) and the Ogallala Aquifer Program, a consortium between USDA-Agricultural Research Service, Kansas State University, Texas AgriLife Research, Texas AgriLife Extension Service, Texas Tech University, and West Texas A&M University.

References:

Alves, I., J.C. Fontes, and L.S. Pereira. 2001. Evapotranspiration estimation from infrared surface temperature. II: The surface temperature as a wet bulb temperature. Trans. of ASAE. 43(3):599-602.

Ben-Gal, A., N. Agam, V. Alchanatis, Y. Cohen, U. Yermiyahu, I. Zipori, E. Presnov, M. Sprintsin, and A. Dag. 2009. Evaluating water stress in irrigated olives: correlation of soil water status, tree water status, and thermal imagery. Irrig. Sci. 27:367-376.

Chaerle, L., I. Leinonen, H.G. Jones, and D. Van Der Straeten. 2006. Monitoring and screening plant populations with combined thermal and chlorophyll imaging. J. of Exp. Botany. 58(4):773-784.

Howell, T.A., J.L. Hatfield, H. Yamada, and K.R. Davis. 1984. Evaluation of Cotton Canopy Temperature to detect crop water stress. Trans. ASAE 27(1):84-88.

Idso, S.B, R.J. Reginato, D.C. Reicosky, and J.L. Hatfield. 1981. Determining soil induced plant water potential depressions in alfalfa by means of infrared thermometry. Agron. J. 73:826-830.

Jones, H.G. 1999. Use of thermography for quantitative studies of spatial and temporal variation of stomatal conductance over leaf surfaces. Plant, Cell and Environment 22, 1043–1055.

Jones, H.G., M. Stoll, T. Santos, C. Sousa, M.M. Chaves, and O.M. Grant. 2002. Use of infrared thermography for monitoring stomatal closure in the field: application to grapevine. J. of Exp. Botany. 53(378): 2249-2260.

Leinonen, I., and H.G. Jones. 2004. Combining thermal and visible imagery for estimating canopy temperature and identifying plant stress. J. of Exp. Botany. 55(401):1423-1431.

Luquet, L., A. Begue, A. Vidal, P. Clouvel, J. Dauzat, A. Olioso, X.F. Gu, and Y. Tao. 2003. Using multidirectional thermography to characterize water status of cotton. Remote Sensing of Env. 84:411-421.

Möeller, M., V. Alchanatis, Y. Cohen, M. Meron, J. Tsipris, A. Naor, V. Ostrovsky, M. Sprintsin, and S. Cohen. 2007. Use of thermal and visible imagery for estimating crop water status of irrigated grapevine. J. of Exp. Botany. 58(4): 827-838.

Peters, R.T. and S.R. Evett. 2004. Modeling diurnal canopy temperature dynamics using one-time-of-day measurements and a reference temperature curve. Agron. J. 96(6): 1553-1561.

Peters, R.T. and S.R. Evett. 2007. Spatial and temporal analysis of crop stress using multiple canopy temperature maps created with an array of center-pivot-mounted infrared thermometers. Trans. ASABE. 50(3):919-927.

Peters, R.T. and S.R. Evett. 2008. Automation of a center pivot using the temperature-time-threshold method of irrigation scheduling. J. Irrig. Drainage Engr., 134 (3):286-290.

Reginato, R.J. 1983. Field quantification of crop water stress. Trans. ASAE 26(3):772-775.

Stoll, M., H.R. Schultz, G. Baecker, and B. Berkelmann-Loehnertz. 2008. Early pathogen detection under different water status and the assessment of spray application in vineyards through the use of thermal imagery. Precision Agric. 9:407-417.

Turner, N.C. 1988. Measurement of plant water status by the pressure chamber technique. Irrig. Sci. (9) 4:289-308.